Geophysical Research Letters

RESEARCH LETTER
10.1029/2020GL089154

Key Points:

- The first semiquantitative estimates of paleorainfall rates from Ca isotope ratios measured in a California stalagmite
- The magnitude of rainfall variability in coastal California during the 8.2 kyr and precursor event approaches/exceeds that of recent decades
- Stalagmite Ca isotope ratios facilitate more direct comparison of paleorainfall with modern climate data, but important questions remain

Supporting Information:

- Supporting Information S1
- Table S1

Correspondence to:
C. B. de Wet,
cameron.de.wet@vanderbilt.edu

Citation:
de Wet, C. B., Erhardt, A. M., Sharp, W. D., Marks, N. E., Bradbury, H. J., Turchyn, A. V., et al. (2021). Semiquantitative estimates of rainfall variability during the 8.2 kyr event in California using speleothem calcium isotope ratios. *Geophysical Research Letters*, *48*, e2020GL089154. https://doi.org/10.1029/2020GL089154

Received 5 JUN 2020
Accepted 17 NOV 2020

Semiquantitative Estimates of Rainfall Variability During the 8.2 kyr Event in California Using Speleothem Calcium Isotope Ratios

Cameron B. de Wet[1], Andrea M. Erhardt[2], Warren D. Sharp[3], Naomi E. Marks[4], Harold J. Bradbury[5], Alexandra V. Turchyn[5], Yiruo Xu[1], and Jessica L. Oster[1]

[1]Department of Earth and Environmental Sciences, Vanderbilt University, Nashville, TN, USA, [2]Department of Earth and Environmental Sciences, University of Kentucky, Lexington, KY, USA, [3]Berkeley Geochronology Center, Berkeley, CA, USA, [4]Lawrence Livermore National Laboratory, Livermore, CA, USA, [5]Department of Earth Sciences, University of Cambridge, Cambridge, UK

Abstract A multiproxy record from a fast-growing stalagmite reveals variable hydroclimate on the California coast across the 8.2 kyr event and a precursor event likely caused by initial drainage of proglacial Lake Agassiz. Using speleothem $\delta^{44}Ca$, we develop the first semiquantitative estimates of paleorainfall variability for California through calibration with measurements of the modern climate and cave environment. We find that the magnitude of rainfall variability during the 8.2 kyr event approached the multiyear variability observable in the recent past (1950–2019) and the magnitude of variability during the precursor event likely exceeded this range. Additionally, we observe other instances of multidecadal variability comparable in magnitude to the precursor event during the record. Our work suggests that speleothem calcium isotope ratios are a powerful semiquantitative means to reconstruct paleorainfall, although numerous factors must be assessed in each cave system before applying this approach.

Plain Language Summary Modeling of future climate suggests that California may experience increased frequency of both extremely wet and extremely dry periods in the 21st century, leading to the emergence of "climate whiplash" phenomena which would significantly stress the state's water-sensitive infrastructure. Understanding hydroclimate changes in California's past can help planners prepare for extremes that may be more severe than those of the historical record. However, existing paleoclimate records are often limited to qualitative interpretations of hydroclimate change, restricting their usefulness. We present new calcium isotope measurements from a California stalagmite that grew from 6,900 to 8,600 years ago, revealing variability in rainfall amounts on the California coast during and surrounding the 8.2 kyr event, an abrupt cold snap noted in other global paleoclimate records 8,200 years ago. We generate semiquantitative estimates of annual rainfall rates during the 8.2 kyr event period and compare them with modern annual rainfall amounts, finding that the magnitude of rainfall variability during and surrounding the 8.2 kyr event approaches and in some cases exceeds that of California today. This work indicates that California may have experienced even more intense "climate whiplash" phenomena in the past than during recent decades, suggesting that future planning may need to consider greater wet and dry extremes.

1. Introduction

Recent modeling indicates that California is likely to experience increased frequency of both wet and dry climate extremes in the 21st century, potentially leading to "climate whiplash" phenomena wherein extremely dry intervals are followed by extremely wet intervals (and vice versa), despite a modest projected change in mean annual precipitation (Swain et al., 2018). While some observations of coupled extreme dry and wet intervals in the last few decades provide examples (e.g., Porter et al., 2011), there is little information in the historic record to assist planners in preparing for the frequency and magnitude of these whiplash events. Paleoclimate records, which indicate large hydroclimatic changes in California's past (e.g., Wise, 2016), may help place constraints on climate-related threats to California's water-sensitive infrastructure.

The abrupt 8.2 kyr climate event represents one of the most extreme perturbations of the Holocene (Thomas et al., 2007) and provides an opportunity to assess the occurrence of "climate whiplash" in California's

paleoclimatic history. In the Northern Hemisphere, the 8.2 kyr event is marked by a ~160 years long cold snap (Alley et al., 1997; Thomas et al., 2007), likely driven by suppression of Atlantic Meridional Overturning Circulation due to increased meltwater flux from the Laurentide Ice Sheet (Matero et al., 2017; Morrill et al., 2013; Wiersma & Renssen, 2006). In response to the 8.2 kyr event, high-resolution speleothem $\delta^{18}O$ records document rapid changes in rainfall in the tropics and monsoon-influenced regions (Cheng et al., 2009), demonstrating the ability of this event to generate widespread perturbations to the global hydrologic cycle. In western North America, there are few archives of sufficient temporal resolution to capture this short-lived event. However, a fast-growing stalagmite from White Moon Cave (WMC) on the central California coast suggests highly variable rainfall during the 8.2 kyr event (Oster et al., 2017), possibly indicating enhanced climate whiplash. This record includes stalagmite $\delta^{18}O$, which responds to moisture source changes, and $\delta^{13}C$, Mg/Ca, and P/Ca that reflect water-rock interactions, flushing from the soil zone, and prior calcite precipitation in the epikarst and cave (PCP). These proxies allow qualitative assessments of rainfall changes. However, each parameter can be influenced by multiple environmental factors that can be challenging to disentangle.

Speleothem calcium isotope ratios ($\delta^{44}Ca$) have emerged as a potentially quantitative proxy for PCP (Li et al., 2018; Magiera et al., 2019; Owen et al., 2016; Reynard et al., 2011), as the lighter isotope (^{40}Ca) preferentially enters the solid phase during carbonate precipitation (Gussone et al., 2005; Tang et al., 2008). The amount of PCP occurring along the water flow path and within the cave is related to rainfall amount, as rapidly infiltrating water will encounter fewer air-filled pore spaces and have less opportunity to degas and precipitate carbonate (Fairchild & Treble, 2009). Here we present new records of Ca ($\delta^{44}Ca$) and Sr ($^{87}Sr/^{86}Sr$) isotopic variability for stalagmite WMC1 covering the early middle Holocene in order to separately reconstruct PCP and water-rock interactions at this site. We further explore the strengths and limitations of speleothem $\delta^{44}Ca$ as a quantitative metric of PCP and paleorainfall and evaluate changes in rainfall surrounding the 8.2 kyr event period in the context of modern rainfall variability in central California.

1.1. Site and Sample Description

White Moon Cave is situated in the late Paleozoic San Vicente marble in the Santa Cruz Mountains east of Davenport, CA (N37°00′, W122°11′; Figure S1a), which is intruded by Cretaceous quartz diorite and overlain by Miocene sandstones and shales. The marble host rock at WMC has variable amounts of accessory mica and contains some Mg (Hart, 1978), and marble with low-mica content dominates the area surrounding the cave. The modern cave entrance lies within a twentieth century quarry that transects the natural cave.

WMC experiences a warm-summer Mediterranean climate and receives on average ~759 mm/yr of precipitation (1950–2016), >80% occurring during the cool season (October-March; Figure S1b). Seasonal temperature variation is small, moderated by the cave's coastal location (11.3–18 °C; Arguez et al., 2010). Rainfall is sourced primarily from winter storms originating in the northern or midlatitude Pacific. However, the region also receives extratropical cyclones that source moisture from the central or eastern tropical Pacific. These systems can develop narrow streams of water vapor concentrated near the surface, termed atmospheric rivers, which are associated with significant flooding in California (Dettinger, 2011).

Stalagmite WMC1 is 25.5 cm tall and was collected >250 m from and ~33 m vertically below the modern cave entrance. The stalagmite grew from ~8,600 until ~239 years cal BP 1950. Only the portion of the stalagmite that grew from ~8,600 to 6,900 years cal BP is discussed here. Dating of this stalagmite by $^{230}Th/U$ chronometry, as well as stable O and C isotope composition and trace element analyses are fully described in Oster et al. (2017).

2. Methods

Sixty-nine ~200 μg samples of calcite were milled along the stalagmite growth axis for $\delta^{44}Ca$ analysis, yielding approximately decadal resolution from ~8,315 to 7,885 years cal BP and multidecadal resolution from ~7,885 to 6,927 and ~8,587 to 8,315 years cal BP. We analyzed the $\delta^{44}Ca$ of 3 marble host rock samples

with variable amounts of accessory mica collected from around the cave, 12 dripwaters and 6 modern calcite samples grown on artificial substrates placed under four drip sites. Drip sites WMC1 and WMC3 are 9–15 m vertically below the modern entrance. Drip sites WMC4 and WMC6 are farther into the cave and ~29 m vertically below the entrance (Figure S2). Artificial substrates installed at each site were retrieved seasonally between 2017 and 2019 (Table S1). Carbonate and water samples were analyzed for $\delta^{44}Ca$ on a ThermoFisher Scientific Triton Plus Thermal Ionization Mass Spectrometer (TIMS) at the Department of Earth Sciences, Cambridge, following the methods of Bradbury and Turchyn (2018). Data are presented in $\delta^{44}Ca$ notation relative to the bulk silicate earth (BSE) standard and are also reported relative to NIST 915A in Table S1. Data were corrected to account for the long-term average drift due to known cup degradation. The average external 2σ over the analysis period on NIST 915B was 0.1‰.

Twenty-nine 5–10 mg samples of speleothem calcite were milled along the growth axis for $^{87}Sr/^{86}Sr$ analysis. Three marble samples (one low-mica, two high-mica) and one sample of quartz diorite were powdered and analyzed for $^{87}Sr/^{86}Sr$. Two soil samples collected at 20-mm and 40-mm depth were progressively leached to characterize the leachable Sr in soil components (supplemental Text S1). Strontium purification was achieved using Eichrom Sr specific resin. Strontium isotopic measurements were performed on a ThermoFisher Scientific Triton TIMS at Lawrence Livermore National Laboratory. Replicate analyses of the NBS-987 Sr standard during the course of this investigation yielded an external reproducibility corresponding to $^{87}Sr/^{86}Sr = 0.710249 \pm 0.000010$ (2σ; $n = 10$).

3. Results

3.1. Speleothem $\delta^{44}Ca$

Stalagmite $\delta^{44}Ca$ values range from −1.20‰ to −0.40‰ BSE (mean = −0.9 ± 0.16‰, $n = 69$) (Figure 1 and Table S1), with variations generally within the 2σ uncertainty of NIST 915B. However, prominent negative, then positive excursions occur prior to the 8.2 kyr event interval at ~8,300 years cal BP, and decadal-scale oscillations are apparent in the middle of the 8.2 kyr event (~8,210-8,130 years cal BP). Stalagmite $\delta^{44}Ca$ then increases steadily from −1.04‰ at ~8,130 years cal BP to −0.81‰ by ~8,013 years cal BP until becoming variable again by ~8,000 years cal BP (Figure 1). Due to lower sampling resolution before ~8,315 and after 7,885 years cal BP, we can only evaluate multidecadal-scale variability, which is low through much of the record, but positive excursions outside of uncertainty occur near ~6,960, ~7,490, ~7,650, and ~7,980 years cal BP.

Modern dripwater $\delta^{44}Ca$ values range from −0.42‰ to −0.14‰ (mean = −0.26 ± 0.07‰, $n = 12$) (all $\delta^{44}Ca$ data given in Figure 2a and Table S1). Dripwater $\delta^{44}Ca$ tends to be less negative in February than June, though often this seasonal variability is smaller than the analytical uncertainty (0.1‰). The $\delta^{44}Ca$ values of modern calcite range from −0.88‰ to −0.68‰ (mean = −0.77 ± 0.08‰, $n = 6$). Measured $\delta^{44}Ca$ for host rocks range from −0.27‰ for the more prevalent low-mica marble to −0.59‰ and −0.49‰ for the two high-mica marbles (mean = −0.45 ± 0.13‰).

3.2. Speleothem $^{87}Sr/^{86}Sr$

Stalagmite $^{87}Sr/^{86}Sr$ values vary between 0.708773 ± 0.000007 and 0.708675 ± 0.000005 (mean = 0.708730 ± 0.00002, $n = 29$) (Figure 1 and Table S1). At a multidecadal sampling resolution, the record displays intervals of relative stability (e.g., ~7,230-6,980 years cal BP) punctuated by excursions outside of analytical uncertainty (e.g., ~8300, ~7835, ~7400 years cal BP). The middle of the 8.2kyr event (~8210-8155 years cal BP) is characterized by higher $^{87}Sr/^{86}Sr$ than the majority of the record. Only one data point outside of the main portion of the 8.2 kyr event displays a more radiogenic value (outside of analytical error) and similar high $^{87}Sr/^{86}Sr$ values occur at ~8,370 and 8,270 years cal BP.

Marble host rocks show significant variability in $^{87}Sr/^{86}Sr$ depending on the prevalence of accessory mica phases. The low-mica marble ($^{87}Sr/^{86}Sr = 0.708428 \pm 0.000007$) is lower (less radiogenic) than the two high-mica marble samples analyzed ($^{87}Sr/^{86}Sr = 0.708916 \pm 0.000006$ and 0.708992 ± 0.000006, respectively).

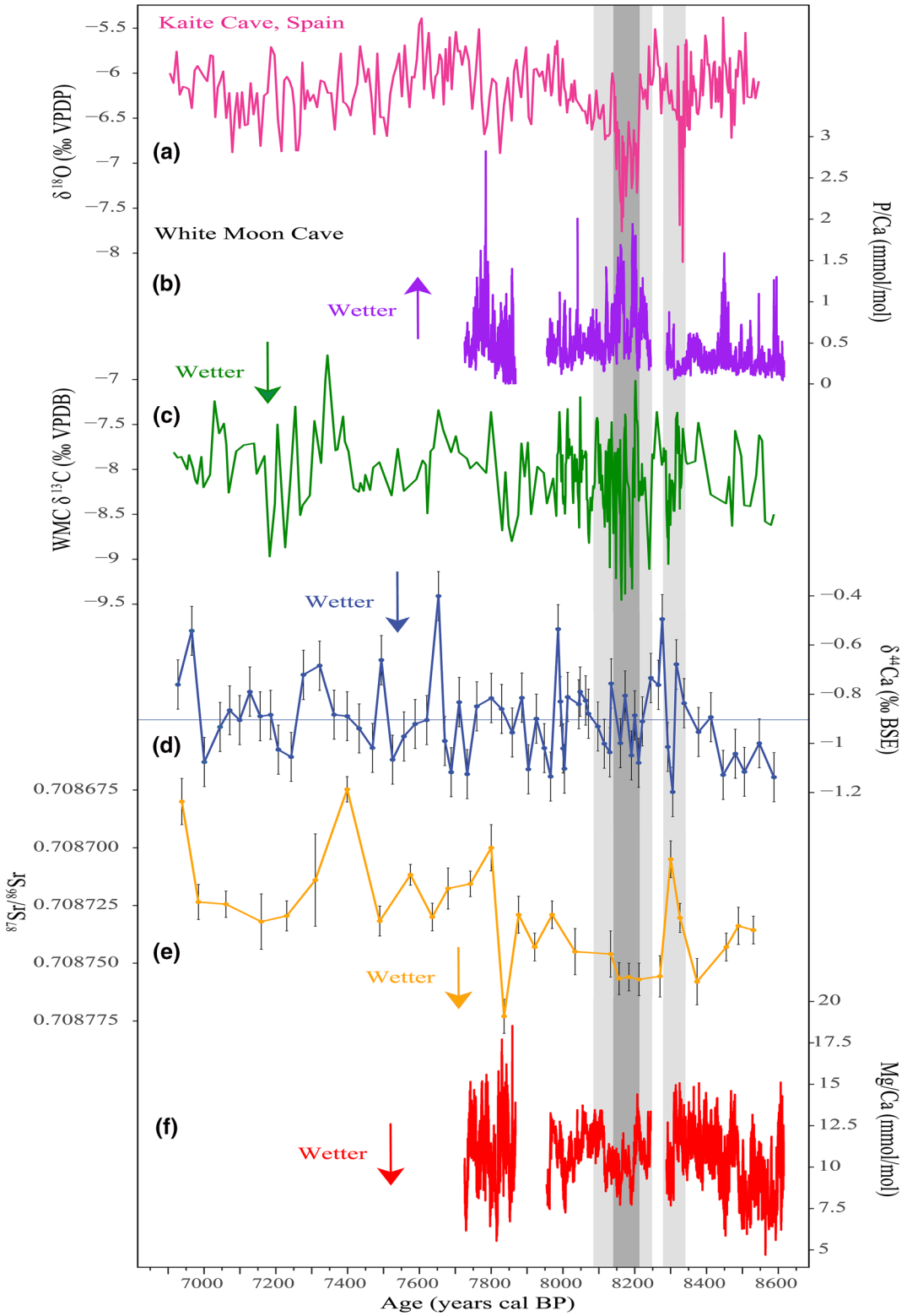

Figure 1. Speleothem $\delta^{18}O$ for Kaite Cave, Spain (a; Dominguez-Villar, 2009), P/Ca (b), $\delta^{13}C$ (c), $\delta^{44}Ca$ (d), $^{87}Sr/^{86}Sr$ (e), and Mg/Ca (f) for WMC1. $\delta^{44}Ca$ error bars show 2σ of the standard NIST915 B over the analysis period (0.1‰). Blue line shows mean $\delta^{44}Ca$ for WMC1. $^{87}Sr/^{86}Sr$ error bars represent the 2σ uncertainty on the measurement (internal reproducibility). Dark and light gray shading show the central portion and entire duration of the 8.2 kyr event after Thomas et al. (2007) and proposed precursor event at ~8,300 years cal BP. WMC, White Moon Cave.

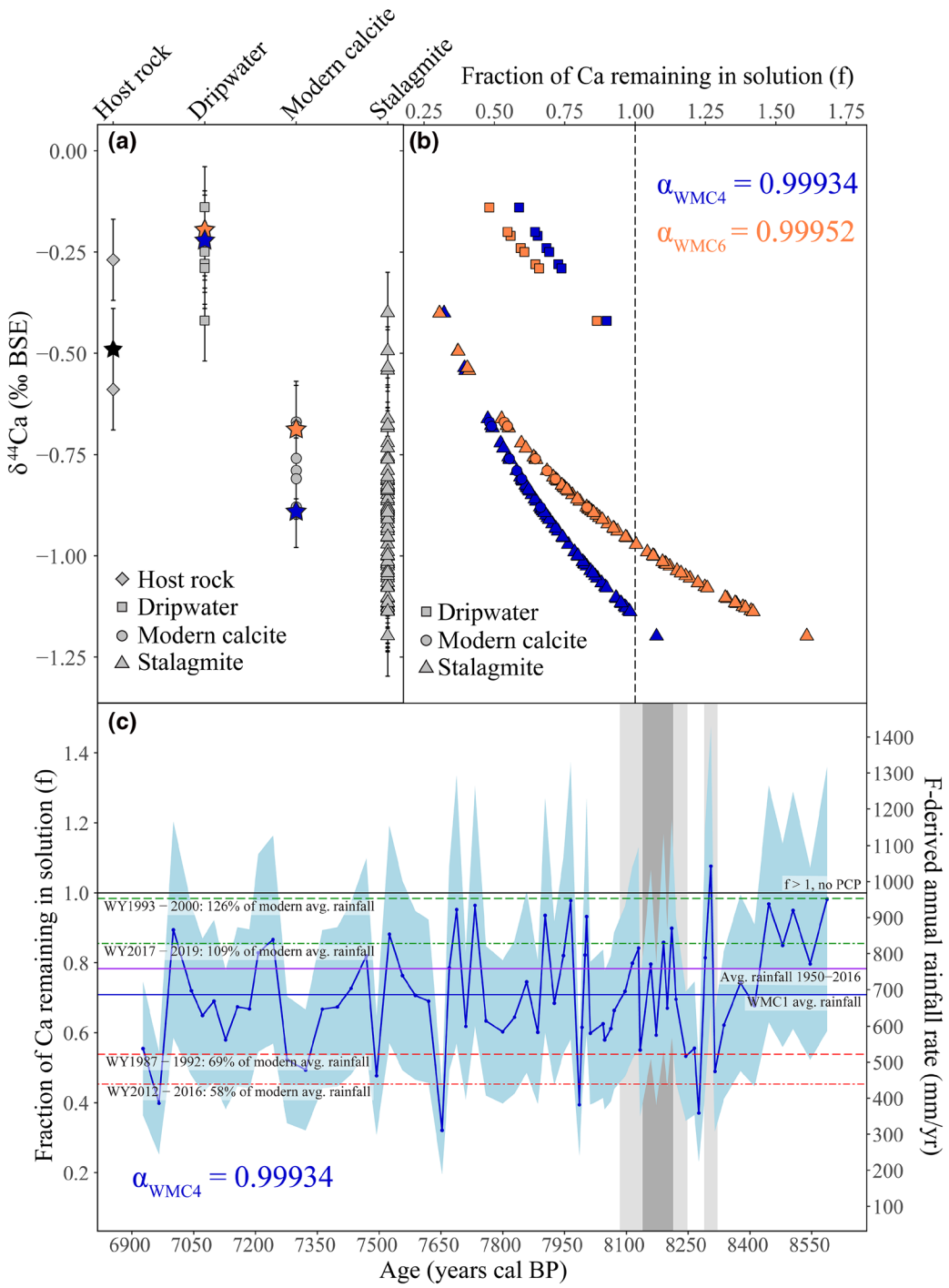

Figure 2. (a) δ^{44}Ca values for WMC host rocks, dripwaters, modern calcite, and stalagmite WMC1. Stars denote median host rock (black) and mean dripwater and modern calcite for WMC4 (blue) and WMC6 (orange) used to calculate *f* values. (b) *f* values calculated using α values from drip site WMC4 (blue) or WMC6 (orange). (c) PCP reconstruction using equation (1) and α_{WMC4}, and estimated rainfall rates. Uncertainty on *f* is analytical uncertainty on δ^{44}Ca measurements propagated using a Monte Carlo approach. $f = 1$ corresponds to a rainfall rate of ~969 mm/yr and represents a threshold above which theoretically no PCP occurs, and no specific rainfall rate can be estimated. Horizontal lines show average rainfall rates for Santa Cruz, CA: WMC1 stalagmite record (blue); annual (January 1950 to January 2020) (purple); water year (WY: October 1 to September 30) 1993–2000 (dashed green); WY 2017–2019 (two-dashed green); WY 1987–1992 (dashed red); WY 2012–2016 (two-dashed red). Description of modern rainfall data in supplemental Text S1. Sources: http://ipm.ucanr.edu/calludt.cgi/WXDESCRIPTION?MAP=&STN=SNTACRUZ.A; https://www.ncdc.noaa.gov/cdo-web/datasets/GHCND/stations/GHCND:USC00047916/detail. WMC, White Moon Cave.

The quartz diorite is more radiogenic than the marbles ($^{87}Sr/^{86}Sr = 0.71019 \pm 0.000008$). Soil leachate $^{87}Sr/^{86}Sr$ increases with depth ($^{87}Sr/^{86}Sr = 0.707787 \pm 0.000006$ at 20 cm and 0.710211 ± 0.000009 at 40 cm).

4. Discussion

4.1. Interpreting Stalagmite $\delta^{44}Ca$ and $^{87}Sr/^{86}Sr$

Speleothem $\delta^{44}Ca$ is uniquely sensitive to PCP. The amount of PCP occurring along the water flow path and within the cave, in turn, is related to the amount of water infiltrating through the epikarst, and thus is linked to rainfall amount (Fairchild & Treble, 2009). For example, more rainfall might lead to a shorter seepage water residence time, fewer air-filled pore spaces, and faster drip rates, supporting less PCP and resulting in dripwaters and speleothems that are less enriched in ^{44}Ca (Li et al., 2018; Magiera et al., 2019; Owen et al., 2016; Tooth & Fairchild, 2003).

During the middle of the 8.2 kyr event (~8,210-8,130 years cal BP) stalagmite $\delta^{44}Ca$ shows decadal-scale oscillations, followed by a steady increase from ~8,130 to ~8,013 years cal BP within the interval of high-resolution sampling (Figure 1). Stalagmite $\delta^{44}Ca$ shows similar variability and moderate correlation ($r_p = 0.39$, $p < 0.001$) with the $\delta^{13}C$ record (Figures 1, S3, and S4), which is also sensitive to PCP and demonstrates rapid, high-amplitude variations during the 8.2 kyr event. However, unlike the $\delta^{13}C$ record, the range of $\delta^{44}Ca$ variability during the 8.2 kyr event is not greater than that observed during other parts of the record. Notably, the largest shifts in $\delta^{44}Ca$ occur prior to the 8.2 kyr event period, at ~8,300 years cal BP.

The calcium isotopic fractionation factor (α) between fluid and calcite is influenced by calcite growth rate, which is partly controlled by saturation state (AlKhatib & Eisenhauer, 2017; Tang et al., 2008). Thus, changes in the speleothem growth rate could affect the recorded speleothem $\delta^{44}Ca$, independent of changes in PCP. Modeled age-depth relationships show that WMC1 growth rate varies by ≤0.01 cm/yr over the course of the record. Tang et al. (2008) found that a tenfold increase in growth rate raises $\Delta^{44}Ca$ by ~0.44‰ at 25 °C, and Owen et al. (2016) estimate that a 360-fold increase would be needed to explain excursions in the Heshang Cave $\delta^{44}Ca$ record. If this sensitivity applies to WMC then the observed growth rate changes are insufficient to explain the magnitude of speleothem $\delta^{44}Ca$ variability. Additionally, WMC1 consists of elongated columnar crystal fabrics intercalated with rare fine layers of silicate detritus. The consistency of this crystal fabric across the stalagmite argues against large changes in $CaCO_3$ saturation that would accompany changes in growth rate (Oster et al., 2017).

Changes in the relative dissolution of marble phases (more or less mica-rich) could influence initial seepage water $\delta^{44}Ca$ values and explain some of the variation in speleothem $\delta^{44}Ca$. However, measured marble $\delta^{44}Ca$ varies by only 0.3‰, whereas the range of variability in the stalagmite is up to 0.8‰. Further, flow path changes that lead to variation in host rock dissolution may be expressed more gradually in the speleothem record. In contrast, PCP can likely increase or decrease quickly, perhaps responding even to interannual changes in effective rainfall. Therefore, changes in host rock dissolution and Ca source likely cannot explain the full range and frequency of variability in the speleothem $\delta^{44}Ca$ record. Likewise, we do not anticipate a measurable contribution of radiogenic ^{40}Ca from dissolution of the micas themselves (Figure S5). The extent of PCP may be influenced by changes in cave ventilation, wherein in stronger ventilation lowers cave air pCO_2 and supports increased PCP within the cave (Ronay et al., 2019). However, at present there is no consistent pattern of seasonal variation in cave air pCO_2, possibly due to the small amplitude of seasonal temperature variations at this coastal location. In contrast, this cave does experience large seasonal variations in drip rate reflecting the strongly seasonal nature of rainfall (Figure S6). Thus, we interpret more negative speleothem $\delta^{44}Ca$ as indicating less PCP in and above the cave, a relatively short seepage residence time, and wetter conditions.

Speleothem $^{87}Sr/^{86}Sr$ displays multidecadal variations in the balance between more and less radiogenic Sr sources (Figure 1). The more prevalent low-mica marble is the most likely less radiogenic end member ($^{87}Sr/^{86}Sr = 0.708428 \pm 0.000007$). The deeper soil ($^{87}Sr/^{86}Sr = 0.710211 \pm 0.000009$) which displays a similar $^{87}Sr/^{86}Sr$ to the diorite situated directly above the cave is most likely the radiogenic endmember. Thus, we interpret higher (more radiogenic) speleothem values as indicating a greater contribution from the deep soil relative to the host rock, reflecting less host rock dissolution, a shorter seepage water residence time, and

wetter conditions (Oster et al., 2009). Conversely, less radiogenic speleothem $^{87}Sr/^{86}Sr$ likely reflects greater relative contribution from the marble driven by longer water residence times and increased marble dissolution during drier conditions. The middle of the 8.2kyr event (~8,210-8,155 years cal BP) is characterized by more radiogenic $^{87}Sr/^{86}Sr$ values relative to the majority of the speleothem record, suggesting increased relative contribution from the deep soil and overall wetter conditions (Figure 1).

4.2. Climate Interpretations During the 8.2 kyr and Precursor Events

Among the proxies analyzed, $\delta^{13}C$ and P/Ca demonstrate the clearest change across the 8.2 kyr event compared to the rest of the record (Figure 1) (Oster et al., 2017). Speleothem P/Ca is associated with soil colloidal material transported into the cave by pulses of water. Peaks in P/Ca during the 8.2 kyr event are coeval with lows in $\delta^{13}C$, consistent with increased influx of soil material during wetter intervals. Speleothem $\delta^{13}C$ is influenced by variable CO_2 degassing and PCP, as the preferential degassing of $^{12}CO_2$ leads to higher residual $\delta^{13}C_{DIC}$ values. The moderate correlation between speleothem $\delta^{13}C$ and $\delta^{44}Ca$ (Figure S3) supports degassing/PCP as an important control on $\delta^{13}C$ in this cave, and the high-frequency variability in $\delta^{13}C$ in the central 8.2kyr event suggests variable PCP during this interval (Figure S4). Comparatively higher amplitude variations in $\delta^{13}C$ than $\delta^{44}Ca$ during the 8.2 kyr event, as well as the corresponding peaks in P/Ca, suggest that PCP-driven changes in $\delta^{13}C$ may be further amplified by soil respiration changes driven by precipitation or temperature changes (Fohlmeister et al., 2020). However, the lower sampling resolution of $\delta^{44}Ca$ may contribute to this difference in the records. In WMC, speleothem Mg/Ca reflects a combination of PCP and changes in dissolution of Mg-rich phases in the host rock, which dissolve more slowly (Oster et al., 2017). Lower Mg/Ca during the 8.2 kyr event is consistent with reduced PCP and less dissolution of Mg-rich phases due to faster infiltration rates. The more radiogenic $^{87}Sr/^{86}Sr$ align with low Mg/Ca values during the central part of the event, also consistent with decreased host rock dissolution relative to soil contributions (Figure 1).

An abrupt, multidecadal shift to wetter conditions beginning ~8,310-8,315 years cal BP is suggested by large shifts in the PCP-sensitive proxies ($\delta^{13}C$, Mg/Ca, and $\delta^{44}Ca$). Conversely, the $^{87}Sr/^{86}Sr$ record shows less radiogenic values at ~8,325 to ~8,299 years cal BP, indicating relatively drier conditions at times that bracket the interval when the other proxies begin to show increasing wetness. This discrepancy may be related to the fact that speleothem $^{87}Sr/^{86}Sr$ is contingent on the movement of a specific volume of water through the epikarst and so may respond more slowly to climate signals than proxies that track PCP, but this is difficult to assess due to the lower sampling resolution of the $^{87}Sr/^{86}Sr$ data. By ~8,270 years cal BP $^{87}Sr/^{86}Sr$ shifts to more radiogenic values, indicating greater relative contribution of Sr from the soil and increased water infiltration. The shift toward wetter conditions in the PCP-sensitive proxies is coincident with a negative excursion between 8,350 and 8,340 years cal BP in the $\delta^{18}O$ record from Kaite Cave, Spain (Domínguez-Villar et al., 2009) within dating uncertainties of both records (±41 years for WMC, ±34 years for Kaite Cave). These shifts may reflect an influx of meltwater to the North Atlantic approximately 100 years prior to the 8.2 kyr event. This pulse of low-$\delta^{18}O$ meltwater from proglacial Lake Agassiz lowers the $\delta^{18}O$ values of Spanish precipitation source waters (Domínguez-Villar et al., 2009). We hypothesize that this meltwater release also led to an abrupt and brief enhancement of the North Pacific storm track through ocean-atmosphere teleconnections.

In sum, proxies that are sensitive to water-rock interactions and soil processes, in addition to PCP, are suggestive of a wetter 8.2 kyr event in coastal California, while $\delta^{44}Ca$, which is specifically sensitive to PCP does not demonstrate a unique response across this interval. $\delta^{13}C$ documents high-amplitude, high-frequency oscillations during the 8.2 kyr event itself, and the more muted response apparent in the $\delta^{44}Ca$ record may reflect the lower sampling resolution of the $\delta^{44}Ca$ that is incapable of resolving these rapid oscillations, or an amplification of the PCP-related $\delta^{13}C$ signal through soil processes. In contrast, $\delta^{44}Ca$, $\delta^{13}C$, and Mg/Ca suggest that the precursor event near 8,300 years cal BP was characterized by an abrupt and short-lived decrease in PCP. The $\delta^{13}C$ demonstrates less volatility within the precursor event, suggesting wetter conditions that were more sustained than during than the 8.2 kyr event itself, a signal that is clearly resolvable in $\delta^{44}Ca$.

4.3. PCP and Rainfall Reconstructions with Ca Isotopes

Speleothem $\delta^{44}Ca$ provides a metric for studying PCP and water infiltration that should be subject to less complex controls than proxies like $\delta^{13}C$ or elemental ratios. Here, we use modern monitoring data to relate $\delta^{44}Ca$ to specific amounts of PCP and assume a linear relationship between PCP and rainfall to generate semiquantitative estimates of rainfall rates during the interval of speleothem growth (Magiera et al., 2019; Owen et al., 2016).

The fraction of the amount of Ca dissolved from the host rock that ultimately remains in solution at the time of speleothem precipitation (f) can be quantified using transfer functions that describe the evolution of Ca isotopes during PCP as a Rayleigh fractionation process (Owen et al., 2016):

$$f = \left(\frac{r_s}{\alpha * r_0} \right)^{\frac{1}{\alpha - 1}} \quad (1)$$

Here, r_s is the Ca isotope ratio in the stalagmite or modern calcite ($r_s = \delta_{CaCO3} / 1000 + 1$), r_0 is the initial Ca isotope ratio in the dripwater ($r_0 = \delta_{dripwater}{}^{f=1}/1{,}000 + 1$), which is assumed to be the same as the measured host rock value, and α is the Ca isotope fractionation factor between calcite and water calculated as:

$$\alpha_{CaCO_3/dripwater} = \frac{1{,}000 + \delta_{CaCO_3}}{1{,}000 + \delta_{dripwater}} \quad (2)$$

We use the measured $\delta^{44}Ca$ of modern calcite precipitated on artificial substrates for δ_{CaCO3} and the measured $\delta^{44}Ca$ of dripwater from the same site for $\delta_{dripwater}$. For each measured speleothem $\delta^{44}Ca$, we use equation (1) with the site-specific α from equation (2) and r_0 calculated from the median $\delta^{44}Ca$ of the host rock to determine f.

Ideally, the Rayleigh model would be calibrated using $\delta^{44}Ca$ data from the same drip site where the stalagmite grew. However, the exact growth location of WMC1 is unknown. Drip sites WMC4 and WMC6 are the most comparable active drip sites for model parametrization because they are located at a similar depth within the cave to the room where WMC1 grew (Figure S1). We use the mean $\delta^{44}Ca$ of WMC4 dripwater from February and June 2019 and the $\delta^{44}Ca$ value from the modern calcite grown at WMC4 between February and June 2019, to calculate a site-specific α_{WMC4} of 0.99934 (Figure 2a). Using equation (2) and data from drip site WMC6, we also calculate a site-specific α_{WMC6} of 0.99952 (Figure 2a). Moving forward, we calibrate the WMC1 stalagmite record using measurements from drip site WMC4 as α_{WMC4} is most similar to that calculated for Heshang Cave ($\alpha = 0.9987$) and Mawmluh Cave ($\alpha = 0.99927$) (Magiera et al., 2019; Owen et al., 2016).

Using α_{WMC4}, WMC4 modern calcite $\delta^{44}Ca$ (−0.89‰), and the median host rock $\delta^{44}Ca$ value (−0.49‰), equation (1) yields an f value of 0.67 for the monitoring period. This implies ~43% of Ca originally dissolved in solution precipitated out along the groundwater flow path before reaching drip site WMC4 during the 5 months that this artificial substrate was placed in the cave. Using this approach and the measured stalagmite $\delta^{44}Ca$ values we calculate f values between 1.08 and 0.32 over the WMC1 record, with one value greater than 1 (Figure 2c). An f value equal to one indicates no Ca has been removed from solution by PCP. Drip logger data for WMC suggest that drip rates within WMC respond quickly to rainfall (Figure S6) so it is possible that there is little opportunity for PCP to occur in this system during large rainfall events. The calculation of f values closes to one likely represents this responsiveness of water flow in the WMC epikarst and the single value greater than one could be explained by analytical uncertainty, as the propagated uncertainty of the f values is quite large. Thus, calculated f values from WMC1 correspond to between 0% (for $f \geq 1$) and 68% Ca removal via PCP over the studied interval (Figure 2c).

To estimate paleorainfall amount from speleothem $\delta^{44}Ca$, we must tie the amount of PCP occurring in the modern system to modern rainfall amount. To make this estimation, we use the rainfall amount measured for Santa Cruz, CA (http://ipm.ucanr.edu/WEATHER/SITES/santacruz.html) from June 8, 2018 to June 8, 2019 (649 mm), encompassing the interval of modern calcite collection. Assuming a linear relationship

between PCP and rainfall amount, speleothem f values can be normalized to the modern rainfall rate, P_{modern} (mm/yr) (Magiera et al., 2019; Owen et al., 2016):

$$P_{paleo} = \frac{P_{modern} * f_{paleo}}{f_{modern}} \quad (3)$$

Here f_{paleo} represents that amount of PCP calculated for each speleothem $\delta^{44}Ca$ value using equation (1), f_{modern} is the amount of PCP calculated for the modern environment using equation (1), and P_{paleo} is the rainfall rate (mm/yr) estimated for each speleothem f value.

Using our modern rainfall calibration, when f_{paleo} equals one, P_{paleo} equals ~969 mm/yr. The one-point normalization yields paleorainfall estimates ranging from ~309 to 969 mm/yr (or greater) during the record, with high-frequency variability between ~870 and 530 mm/yr (~115-68% of modern average annual rainfall), during the core of the 8.2 kyr event (Figure 2c).

Although these are only semiquantitative estimates of paleorainfall, normalizing the approximations of PCP to modern rainfall amounts in this way provides a first approximation of the magnitude of change in past climate (how much wetter/drier), as opposed to the direction of change alone (wetter versus drier) and supports comparisons with recent precipitation variability. We compare the reconstructed rainfall estimates for WMC1 with the average annual rainfall for Santa Cruz, CA, from two recent intervals characterized by extreme dryness preceding extreme wetness (Wang et al., 2017): water years 1987–1992 (522 mm/yr) followed by water years 1993–2000 (953 mm/yr) and water years 2012–2016 (439 mm/yr) followed by water years 2017–2019 (828 mm/yr) (Figure 2c and supplemental Text S1). We find that the magnitude of rainfall variability during the 8.2 kyr event (68–115% of modern average) is less than that of the 1990s (69–126%) or 2010s (58–109%). However, the magnitude of variability during the precursor event (~8,300 years cal BP) (63 ≥ 128%) and other excursions within our record exceeds that of the instrumental record (Figure 2c). Thus, this semiquantitative reconstruction of (sub)decadal rainfall variability demonstrates that during the early middle Holocene, California may have experienced climate variability that was comparable to or greater than that of the last few decades.

While this method shows promise for semiquantitative rainfall reconstructions, its application is complicated by potential variability in the $\delta^{44}Ca$ of the host rock, water mixing, and mineral dissolution/precipitation rates. Calculated f values will vary depending on host rock $\delta^{44}Ca$ (Figure S7b) and as a function of α value (Figure 2b). This sensitivity underscores the importance of constraining variability in $\delta^{44}Ca$ across the host rock and among drip sites and emphasizes that, when possible the model must be optimized for each speleothem. Here, we accomplish this by using the median $\delta^{44}Ca$ from a range of host rock samples and an α value for a drip site most similar in depth beneath the surface to stalagmite WMC1, noting that depth within the cave can lead to variations in seepage water travel time that can influence PCP (Figure 2b). Lastly, the linear relationship between PCP and rainfall amount in the modern must be further evaluated over longer timescales and throughout cave environments to determine its accuracy and applicability for producing semiquantitative estimates of paleorainfall across multiple climate regimes.

5. Conclusions

New speleothem $\delta^{44}Ca$ and $^{87}Sr/^{86}Sr$ records document variable infiltration and overall wetter conditions, respectively, during the 8.2 kyr event relative to much of the rest of our record. As a uniquely sensitive proxy of PCP, our $\delta^{44}Ca$ record indicates that soil respiration may have amplified the PCP response to increased infiltration in the $\delta^{13}C$ record. This new record of PCP substantiates the hypothesis that a precursor event influenced California climate ~100 years prior to the 8.2 kyr event, resulting in larger changes in rainfall than the event itself. This observation, as well as that of positive excursions in $\delta^{44}Ca$ after the 8.2 kyr event, point toward "climate whiplash"-type phenomena in coastal California under early Holocene boundary conditions, potentially in response to freshwater and other forcings. We show that speleothem $\delta^{44}Ca$ and $^{87}Sr/^{86}Sr$ provide valuable proxies for infiltration rates that can be incorporated in a multiproxy approach to better characterize local paleorainfall signals.

We use stalagmite and modern cave system $\delta^{44}Ca$, normalized to modern rainfall, to generate the first semiquantitative estimates of paleorainfall change in California from speleothems. Using this approach, we find

that the magnitude of paleorainfall variation during the 8.2 kyr event approached the multiyear variability observed in recent decades in California, while that of the precursor event and three other intervals exceeded recent variability. Although new insights and semiquantitative estimates of past rainfall can be generated from speleothem $\delta^{44}Ca$, we show that numerous factors must be assessed before this technique can be applied in a given cave system. These include a better understanding of variability in host rock $\delta^{44}Ca$ and spatial controls on Ca isotope cycling in the epikarst. A thorough evaluation of the relationship between PCP and rainfall in modern cave environments will be especially important. Nonetheless, the quantification of PCP variability and past rainfall rates using speleothem $\delta^{44}Ca$ offers a promising tool for estimating the magnitude of changes in past hydroclimate.

Acknowledgments
Funding was provided by the National Science Foundation (AGS-1554998) and the National Geographic Society (NGS-39815) (to Jessica L. Oster) and the Karst Waters Institute and the Geological Society of America (to Cameron B. de Wet). Calcium isotope analyses were supported through ERC StG 307582 CARBONSINK (to Alexandra V. Turchyn) and NERC NE/R013519/1 (to Harold J. Bradbury). We thank Mike Davies and Bruce Rogers of the Western Cave Conservancy for guidance in the field and the editor, Stacy Carolin, and two other anonymous reviewers for constructive feedback. Data are with the NOAA National Centers for Environmental Information Paleoclimatology Data repository (https://www.ncdc.noaa.gov/paleo/study/32012). This work was performed under the auspices of the U.S. Department of Energy by Lawrence Livermore National Laboratory under Contract DE-AC52-07NA27344. LLNL-JRNL-807062.

References

AlKhatib, M., & Eisenhauer, A. (2017). Calcium and strontium isotope fractionation in aqueous solutions as a function of temperature and reaction rate; I. Calcite. *Geochimica et Cosmochimica Acta*, *209*, 296–319. https://doi.org/10.1016/J.GCA.2016.09.035

Alley, R. B., Mayewski, P. A., Sowers, T., Stuiver, M., Taylor, K. C., & Clark, P. U. (1997). Holocene climatic instability: A prominent, widespread event 8200 yr ago. *Geology*, *25*, 483–486. https://doi.org/10.1130/0091-7613(1997)025%3C0483:HCIAPW%3E2.3.CO

Arguez, A., Durre, I., Applequist, S., Squires, M., Russell Vose, R., Yin, X., & Bilotta, R. (2010). *NOAA's U.S. Climate Normals (1981–2010)*. Santa Cruz, CA: NOAA National Centers for Environmental Information. https://doi.org/10.7289/V5PN93JP

Bradbury, H. J., & Turchyn, A. V. (2018). Calcium isotope fractionation in sedimentary pore fluids from ODP Leg 175: Resolving carbonate recrystallization. *Geochimica et Cosmochimica Acta*, *236*, 121–139. https://doi.org/10.1016/j.gca.2018.01.040

Cheng, H., Fleitmann, D., Edwards, R. L., Wang, X., Cruz, F. W., Auler, A. S., et al. (2009). Timing and structure of the 8.2 kyr B.P. event inferred from δ18O records of stalagmites from China, Oman, and Brazil. *Geology*, *37*, 1007–1010. http://doi.org/10.1130/G30126A.1

Dettinger, M. (2011). Climate change, atmospheric rivers, and floods in California—A multimodel analysis of storm frequency and magnitude changes. *Journal of the American Water Resources Association*, *47*, 514–523. https://doi.org/10.1111/j.1752-1688.2011.00546.x

Domínguez-Villar, D., Fairchild, I. J., Baker, A., Wang, X., Edwards, R. L., & Cheng, H. (2009). Oxygen isotope precipitation anomaly in the North Atlantic region during the 8.2 ka event. *Geology*, *37*, 1095–1098. https://doi.org/10.1130/G30393A.1

Fairchild, I. J., & Treble, P. C. (2009). Trace elements in speleothems as recorders of environmental change. *Quaternary Science Reviews*, *28*, 449–468. https://doi.org/10.1016/j.quascirev.2008.11.007

Fohlmeister, J., Voarintsoa, N. R. G., Lechleitner, F. A., Boyd, M., Brandstätter, S., Jacobson, M. J., & Oster, J. L. (2020). Main controls on the stable carbon isotope composition of speleothems, *Geochimica et Cosmochimica Acta*, *279*, 67–87. https://doi.org/10.1016/j.gca.2020.03.042

Gussone, N., Böhm, F., Eisenhauer, A., Dietzel, M., Heuser, A., Teichert, B. M. A., et al. (2005). Calcium isotope fractionation in calcite and aragonite: *Geochimica et Cosmochimica Acta*, *69*, 4485–4494. https://doi.org/10.1016/j.gca.2005.06.003

Hart, E. W. (1978). Limestone, Dolomite, and Shell Resources of the coast ranges Province, California (Bulletin 197).Sacramento, CA: California Division of Mines and Geology Bulletin.

Li, X., Cui, X., He, D., Liao, J., & Hu, C. (2018). Evaluation of the Heshang Cave stalagmite calcium isotope composition as a paleohydrologic proxy by comparison with the instrumental precipitation record. *Scientific Reports*, *8*, 2615. https://doi.org/10.1038/s41598-018-20776-5

Magiera, M., Lechleitner, F. A., Erhardt, A. M., Hartland, A., Kwiecien, O., Cheng, H., et al (2019). Local and regional Indian summer monsoon precipitation dynamics during termination II and the last interglacial. *Geophysical Research Letters*, *46*, 12454–12463. https://doi.org/10.1029/2019GL083721

Matero, I. S. O., Gregoire, L. J., Ivanovic, R. F., Tindall, J. C., & Haywood, A. M. (2017). The 8.2 ka cooling event caused by Laurentide ice saddle collapse. *Earth and Planetary Science Letters*, *473*, 205–214. https://doi.org/10.1016/j.epsl.2017.06.011

Morrill, C., Legrande, A. N., Renssen, H., Bakker, P., & Otto-Bliesner, B. L. (2013). Model sensitivity to North Atlantic freshwater forcing at 8.2 ka. *Climate of the Past*, *9*, 955–968. https://doi.org/10.5194/cp-9-955-2013

Oster, J. L., Montañez, I. P., Sharp, W. D., & Cooper, K. M. (2009). Late Pleistocene California droughts during deglaciation and Arctic warming. *Earth and Planetary Science Letters*, *288*, 434–443. https://doi.org/10.1016/j.epsl.2009.10.003

Oster, J. L., Sharp, W. D., Covey, A. K., Gibson, J., Rogers, B., & Mix, H. (2017). Climate response to the 8.2 ka event in coastal California. *Scientific Reports*, *7*, 3886. https://doi.org/10.1038/s41598-017-04215-5

Owen, R. A., Day, C. C., Hu, C. Y., Liu, Y. H., Pointing, M. D., Blättler, C. L., & Henderson, G. M. (2016). Calcium isotopes in caves as a proxy for aridity: Modern calibration and application to the 8.2 kyr event. *Earth and Planetary Science Letters*, *443*, 129–138. https://doi.org/10.1016/j.epsl.2016.03.027

Porter, K., Wein, A., Alpers, C., Baez, A., Barnard, P., Carter, J., et al. (2011). *Overview of the ARkStorm Scenario (Rep. No. 2010-1312)*. Reston, VA: United States Geological Survey.

Reynard, L. M., Day, C. C., & Henderson, G. M. (2011). Large fractionation of calcium isotopes during cave-analogue calcium carbonate growth. *Geochimica et Cosmochimica Acta*, *75*, 3726–3740. https://doi.org/10.1016/j.gca.2011.04.010

Ronay, E. R., Breitenbach, S. F. M., & Oster, J. L. (2019). Sensitivity of speleothem records in the Indian Summer Monsoon region to dry season infiltration. *Scientific Reports*, *9*, 5091. https://doi.org/10.1038/s41598-019-41630-2

Swain, D. L., Langenbrunner, B., Neelin, J. D., & Hall, A. (2018). Increasing precipitation volatility in twenty-first-century California. *Nature Climate Change*, *8*, 427–433. https://doi.org/10.1038/s41558-018-0140-y

Tang, J. W., Dietzel, M., Bohm, F., Kohler, S. J., & Eisenhauer, A. (2008). Sr^{2+}/Ca^{2+} and Ca^{44}/Ca^{40} fractionation during inorganic calcite formation: II. Ca isotopes. *Geochimica et Cosmochimica Acta*, *72*, 3733–3745. https://doi.org/10.1016/j.gca.2008.05.033

Thomas, E., Wolff, E. W., Mulvaney, R., Steffensen, J. P., Johnsen, S. J., Arrowsmith, C., et al. (2007). The 8.2 ka event from Greenland ice cores: *Quaternary Science Reviews*, *26*, 70–81. https://doi.org/10.1016/j.quascirev.2006.07.017

Tooth, A. F., & Fairchild, I. J. (2003). Soil and karst aquifer hydrological controls on the geochemical evolution of speleothem-forming drip waters, Crag Cave, southwest Ireland. *Journal of Hydrology*, *273*, 51–68. https://doi.org/10.1016/S0022-1694(02)00349-9

Wang, S.-Y. S., Yoon, J.-H., Becker, E., & Gillies, R. (2017). California from drought to deluge. *Nature Climate Change*, *7*, 465–468. https://doi.org/10.1038/nclimate3330

Wiersma, A. P., & Renssen, H. (2006). Model–data comparison for the 8.2kaBP event: Confirmation of a forcing mechanism by catastrophic drainage of Laurentide Lakes. *Quaternary Science Reviews*, *25*, 63–88. https://doi.org/10.1016/j.quascirev.2005.07.009

Wise, E. K. (2016). Five centuries of U.S. West Coast drought: Occurrence, spatial distribution, and associated atmospheric circulation patterns. *Geophysical Research Letters*, *43*, 4539–4546. https://doi.org/10.1002/2016GL068487

Reference From the Supporting Information

Ryu, J.-S., Jacobson, A. D., Holmden, C., Lundstrom, C., & Zhang, Z. (2011). The major ion, δ44/40Ca, δ44/42Ca, and δ26/24Mg geochemistry of granite weathering at pH=1 and T=25°C: Power-law processes and the relative reactivity of minerals. *Geochimica et Cosmochimica Acta*, *75*, 6004–6026.